Local structures and concentration dependence of magnetic properties in Cr- and Mn-doped amorphous silicon ferromagnetic thin films

Y. L. Soo,[1,2,][*] J. H. Yao,[3] C. S. Wang,[1] S. L. Chang,[1] C. A. Hsieh,[2] J. F. Lee,[2] and T. S. Chin[3,4]

[1]*Department of Physics, National Tsing Hua University, Hsinchu 30013, Taiwan*
[2]*National Synchrotron Radiation Research Center, Hsinchu, Taiwan*
[3]*Department of Materials Science and Engineering, National Tsing Hua University, Hsinchu 30013, Taiwan*
[4]*Department of Materials Science and Engineering, Feng Chia University, Taichung 40724, Taiwan*

Local environments surrounding magnetic ions in Mn- or Cr-doped and hydrogenated amorphous Si films have been determined using extended x-ray absorption fine structure (EXAFS) method. These films are found to be ferromagnetic with high Curie temperatures above 250 K and therefore are of tremendous interest for practical spintronics applications. Our EXAFS results indicate that these material systems are nearly free of dopant clusters and oxides up to an unusually high dopant concentration of 20–22 at. %. As the dopant concentration increases, the saturation magnetization in the Cr-doped samples is decreased while that in the Mn-doped sample remains practically unchanged. Antiferromagnetic coupling of magnetic ions and enhancement of carrier-mediated ferromagnetism are proposed to account for the different concentration dependence of magnetization in the Cr- and Mn-doped samples.

Ferromagnetic semiconductors are of pivotal importance for the development of semiconductor spintronics.[1,2] Apart from III–V diluted magnetic semiconductors (DMS), which have been extensively studied during the past decades, group IV DMSs such as Mn-doped Ge and Si have recently attracted considerable interest.[3–6] Owing to their compatibility with Si-based semiconductor industry, group IV ferromagnetic DMSs are especially suited for constructing spin-injecting components to be incorporated into existing electronic devices. High Curie temperatures above room temperature have been reported in both Mn- and Cr-doped Si making this class of materials promising candidates for practical spintronic applications. To increase the solubility of magnetic ions in Si, hydrogenated amorphous silicon has also been used to replace the crystalline Si host and results in improved magnetic properties.[7,8]

However, the usefulness of DMSs in spintronics as spin-polarized current injector relies not only on the apparent ferromagnetism of the materials but also on the detailed structure of the magnetic ions in the semiconductor host. Formation of magnetic clusters or phase separation in the matrix materials may dominate the ferromagnetism of the DMS while lacking direct effects on the itinerant carriers in the host. In addition, we note that practical applications of amorphous semiconductors in spintronics are also challenged by spin-conserving problems in spin injection. Since the magnetic dopant atoms in general do not possess long-range structural order, x-ray or neutron diffraction is not useful for probing the locations of magnetic ions in the semiconductor host. On the other hand, the short-range-order method of extended x-ray absorption fine structure (EXAFS) is uniquely suited for this purpose.[9–13] In the present work, we employed the EXAFS technique to probe the local structures surrounding magnetic Mn and Cr atoms in ferromagnetic Mn-doped and Cr-doped amorphous Si thin-film samples prepared by magnetron co-sputtering method. In such materials, not only the dopant but also the host does not have long-range structural order. The local structural information obtained from EXAFS analysis appears to be especially important. All the amorphous Si thin films used in this work have been hydrogenated. It is reported in previous EXAFS literature that hydrogenation can reduce the disorder and distortion either intrinsic or induced by incorporation of impurities in semiconductor materials.[14–17]

Samples of Mn- and Cr-doped amorphous silicon (a-Si) thin films of thickness 200 nm were deposited by rf magnetron cosputtering technique at room temperature on glass and Si substrates. To eliminate the dangling bonds which can trap dopants/carriers and therefore degrade the electronic and magnetic properties, these films were hydrogenated using a sputtering gas mixture of 20% H_2 in Ar during the growth. Four Mn-doped and four Cr-doped samples were selected for the EXAFS measurements. The concentrations of Mn in the Mn-doped samples are 10.5, 15.5 and 20.0 at. %, respectively. The Cr concentrations in the Cr-doped films are 8.0, 14.0, 18.0, and 22.0 at. %, respectively. The Mn or Cr concentration was determined using the field-emission electron-probe microanalysis (FE-EPMA) method. One of the a-$Si_{0.895}Mn_{0.105}$:H samples was annealed at 100 °C for 10 min to verify its thermal stability. High-resolution transmission electron micrographs (HRTEM) confirm that the samples are indeed amorphous and free from precipitates.[7,8] The ferromagnetism of the films was investigated by superconducting quantum interference device (SQUID) measurements which exhibit clear ferromagnetic hysteresis loops for all samples at 10 K (see Refs 7 and 8 and Fig. 1). The Curie temperatures were determined by the crossing point of field-cooled (FC) and zero-field-cooled (ZFC) magnetization versus temperature (M-T) curves to be higher than 250 K and room temperature for the Mn- and Cr-doped samples, respectively.[7,8]

The Mn and Cr K-edge EXAFS measurements were carried out in fluorescence mode of detection at Beamline 17C of Taiwan Light Source (TLS) at National Synchrotron Ra-
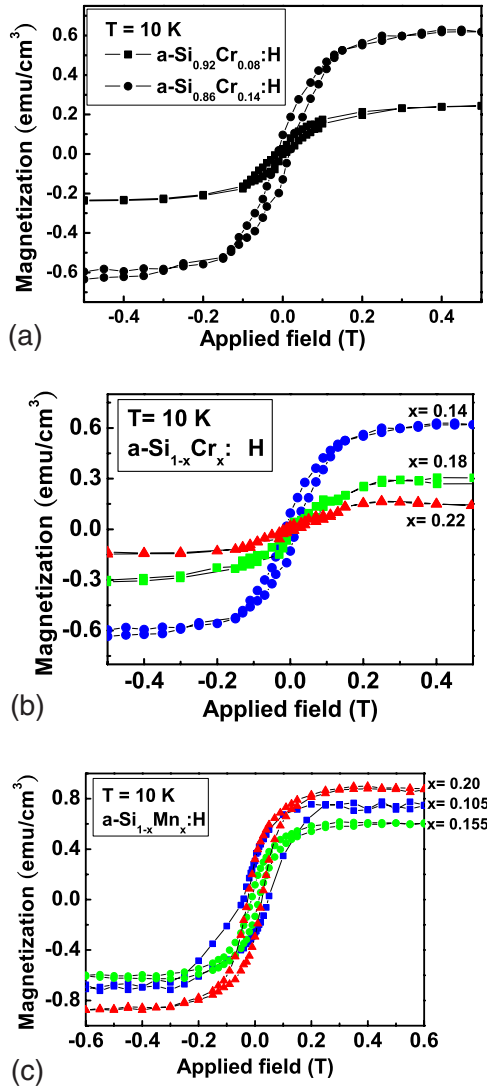
FIG. 1. (Color online) The SQUID data of a Cr-doped and a Mn-doped amorphous Si films. (a) A comparison of M-H curves for Cr-doped samples with different dopant concentrations. (b) A comparison of M-H curves for Cr-doped samples with different dopant concentrations. (c) A comparison of M-H curves for Mn-doped samples with different dopant concentrations.

diation Research Center (NSRRC), Hsinchu, Taiwan. An energy dispersive single element Si(Li) detector and a Lytle fluorescence detector were used to collect x-ray fluorescence photons from the Cr- and Mn-doped samples, respectively. A well-known data reduction program was used to extract the EXAFS χ functions from the raw experimental data.[18] The χ functions of the Cr- and Mn-doped samples are then Fourier-transformed into real space plotted as fine lines in Figs. 2 and 3, respectively. Local structural parameters were quantitatively extracted from the χ functions using an improved curve-fitting procedure[12] with back scattering amplitude and phase shifts functions obtained from the FEFF software.[19] In the curve-fitting process, k ranges of 3.0–11.0 Å^{-1} and 3.0–9.0 Å^{-1} and R ranges of 1.54–2.36 Å and 1.34–2.52 Å were adopted for the Mn-doped samples and the Cr-doped samples, respectively. The degrees of freedom
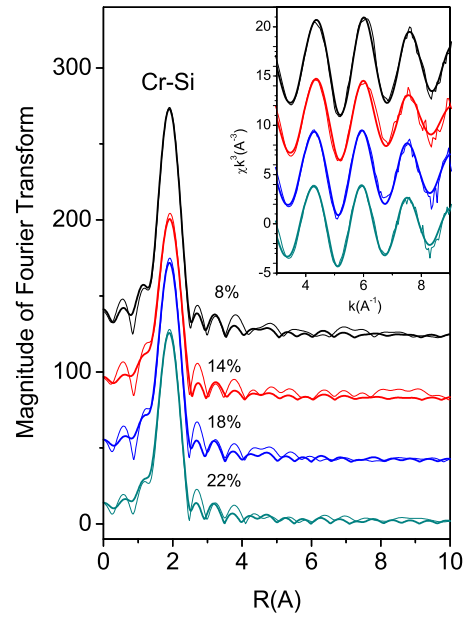

FIG. 2. (Color online) Cr K-edge EXAFS data for the Cr-doped samples. Fine lines: experimental; Coarse lines: curve fitting. Curves have been shifted vertically for the sake of clarity (from top: a-Si$_{0.92}$Cr$_{0.08}$:H, a-Si$_{0.86}$Cr$_{0.14}$:H, a-Si$_{0.82}$Cr$_{0.18}$:H, and a-Si$_{0.78}$Cr$_{0.22}$:H).

for the Fourier-filtered spectra is thus estimated to be 6,[20] which is sufficient for extracting all the required fitting parameters from the Fourier-filtered data. The amplitude reduction factor S$_0{}^2$ representing the central atom shake-up and shake-off effects was set to be 0.8 for Mn and 0.73 for Cr as determined in previous papers.[10,21] The final values of fitting
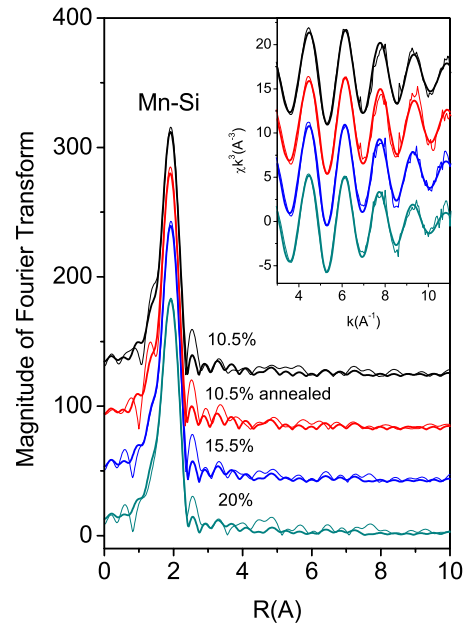

FIG. 3. (Color online) Mn K-edge EXAFS data for the Mn-doped samples. Fine lines: experimental; Coarse lines: curve fitting. Curves have been shifted vertically for the sake of clarity (from top: a-Si$_{0.895}$Mn$_{0.105}$:H, a-Si$_{0.895}$Mn$_{0.105}$:H annealed, a-Si$_{0.845}$Mn$_{0.155}$:H, and a-Si$_{0.8}$Mn$_{0.2}$:H).

TABLE I. Parameters of local structure around Cr atoms obtained from curve-fitting of the Cr K-edge EXAFS. N is the coordination number. R is the bond length. σ^2 is the Debye-Waller-like factor serving as a measure of local disorder. ΔE_0 is the difference between the zero kinetic energy value of the sample and that of the theoretical model used in FEFF. Uncertainties were estimated by the double-minimum residue $(2\chi^2)$ method.

Sample	Bond	N	R (Å)	σ^2 (10^{-3} Å^2)	ΔE (eV)
a-Si$_{0.92}$Cr$_{0.08}$:H	Cr-Si	5.7 ± 0.2	2.405 ± 0.005	9.4 ± 0.4	-2.1 ± 0.5
a-Si$_{0.86}$Cr$_{0.14}$:H	Cr-Si	5.7 ± 0.3	2.417 ± 0.005	13 ± 1	-1.2 ± 0.5
a-Si$_{0.82}$Cr$_{0.18}$:H	Cr-Si	5.3 ± 0.2	2.418 ± 0.005	10.3 ± 0.8	-3.4 ± 0.5
a-Si$_{0.78}$Cr$_{0.22}$:H	Cr-Si	5.0 ± 0.3	2.416 ± 0.005	10.4 ± 1.0	-4.2 ± 0.5

parameters for the Cr-doped and Mn-doped samples are listed in Tables I and II, respectively.

As shown in Figs. 2 and 3, the Fourier transforms of χ functions for the Cr-doped and Mn-doped films exhibit only one pronounced peak attributed to the nearest neighboring shell from the absorbing dopant atoms. The absence of prominent peaks from more remote shells indicates the lack of long-range structural order around the central dopant atoms. Hence, we exclude the possibility of crystalline phases forming around the dopant atoms in these amorphous Si samples. As shown in Tables I and II, the pronounced peak in the Fourier transform for all Cr-doped and Mn-doped samples is identified by curve-fittings to represent a Si nearest shell around the dopant atoms. The coordination number (N) and interatomic distance (R) for this (Si) neighboring shell are 5.0–5.7 and 2.405–2.418 Å for the Cr-doped samples, respectively. N and R of the Mn-doped samples are 4.9–6.1 and 2.352–2.368 Å, respectively. It is obvious that no structural order beyond the nearest neighboring shell surrounding the dopant atoms are present in these doped amorphous Si thin films. These results demonstrate that incorporation of Cr and Mn in hydrogenated amorphous Si thin films can be achieved nearly free of magnetic ion clusters and oxides even up to an unusually high dopant concentration of 20–22 at. %.

We note that the observed Mn-Si and Cr-Si bond lengths (on average 2.361 Å and 2.414 Å, respectively) are close to the Si-Si bond length of 2.351 Å in the diamondlike Si structure indicating that Cr or Mn dopants most likely substitute for Si atoms in the amorphous samples. However, the average coordination numbers of the first (Si) shell, 4.9–6.1 for Mn atoms and 5.0–5.7 for Cr atoms, are appreciably higher than the substitutional value of 4.0 in crystalline Si.

We note that the coordination number is highly correlated with the amplitude reduction factor S_0^2 and the mean-square displacement σ^2. It is widely accepted that the uncertainty for coordination number can be as high as 20% in the EXAFS analysis which is much higher than the uncertainty estimated by the standard double-minimum residue $(2\chi^2)$ method. On the other hand, although it is highly questionable for a substitutional dopant atom to have more than four nearest neighboring Si atoms in *crystalline* samples, one or two additional Si atoms around the dopants should be reasonable for *amorphous* samples due to extra free volume in their distorted structure. Moreover, the tetrahedral and hexagonal interstitials in the crystalline Si that can complicate the EXAFS analysis[22] simply do not exist in the amorphous Si structure which is basically comprised of continuous random network of tetrahedrally bonded Si atoms in the short-range-order regime. Such distorted random network in amorphous Si possesses a lot of free volume that can accommodate a great deal of solute atoms including transition metals, up to a concentration much higher (e.g., 17.5 at. % by e-beam evaporation in one report)[23] than those normally found in crystalline Si (very small concentration of less than 1 at. %). Our samples were hydrogenated and thus may dissolve even more solute atoms.

The local structural parameters listed in Tables I and II also reveal weak dependence of average local environment on the dopant concentration. As shown in Table I, the coordination number of the nearest Si shell around Cr slightly decreases as the concentration of Cr increases from 8.0 to 22 at. %. A reverse trend of change in Si-shell coordination number around Mn-dopant atoms was found in the Mn-doped films (see Table II). As the Mn concentration increases from 10.5 to 20 at. %, the coordination number increases

TABLE II. Parameters of local structure around Mn atoms obtained from curve-fitting of the Mn K-edge EXAFS

Sample	Bond	N	R (Å)	σ^2 (10^{-3} Å^2)	ΔE (eV)
a-Si$_{0.895}$Mn$_{0.105}$:H	Mn-Si	5.2 ± 0.2	2.358 ± 0.005	8.7 ± 0.4	-0.6 ± 0.5
a-Si$_{0.895}$Mn$_{0.105}$:H annealed	Mn-Si	4.9 ± 0.3	2.352 ± 0.005	7.8 ± 0.6	-1.5 ± 0.5
a-Si$_{0.845}$Mn$_{0.155}$:H	Mn-Si	5.8 ± 0.2	2.365 ± 0.005	10.0 ± 0.4	-0.3 ± 0.5
a-Si$_{0.8}$Mn$_{0.2}$:H	Mn-Si	6.1 ± 0.2	2.368 ± 0.005	11.0 ± 0.3	-0.3 ± 0.5

from 5.2 ± 0.2 to 6.1 ± 0.2 accompanied by an increase in Mn-Si bond length from 2.358 ± 0.005 to 2.368 ± 0.005 Å.

It is worth noting that the saturation magnetization of the Cr-doped samples first increases from 0.24 to 0.63 emu/cc and then decreases to 0.31 emu/cc and 0.16 emu/cc as the concentration of Cr is increased from 8.0 to 14.0 at. % and then to 18.0 and 22.0 at. %, respectively [Figs. 1(a) and 1(b)]. On the other hand, appreciable variation in saturation magnetization was not found in the Mn-doped samples. As the Mn concentration is increased from 10.5 to 15.5 at. % and then to 20 at. %, the saturation magnetization stays at close values of 0.77, 0.60, and 0.82 emu/cc, respectively [Fig. 1(c)]. Annealing of the 10.5 at. % sample at 100 °C for 10 min only slightly increases the saturation magnetization to 0.92 emu/cc with decreased average coordination number and bond length.

Our EXAFS results show that both Mn and Cr dopants are incorporated in amorphous silicon samples without forming detectable Mn-Mn or Cr-Cr clusters and therefore exclude the possibility of dominant direct exchange interaction between magnetic ions in either case. As demonstrated in Refs. 7 and 8, indirect exchange interaction of the RKKY and the fitted percolation of magnetic polarons models are considered to account for the magnetism in the Mn-doped and Cr-doped samples, respectively. Based on our present data of magnetic measurements, we propose that antiferromagnetic coupling such as superexchange between magnetic ions may appear as the dopant concentration increases and therefore reduces the saturation magnetization. Similar effects of antiferromagnetism due to direct dopant-dopant interaction have been reported in several transition metal doped oxides such as the Co-doped ZnO system.[24,25] The obvious decrease in magnetization in the Cr-doped samples as the Cr concentration increases from 14.0 to 22.0 at. % can be attributed to such effect. However, apparent variation in saturation magnetization was not found in the Mn-doped samples. We note, from Refs. 7 and 8, a small Cr peak in the x-ray diffraction (XRD) patterns started to appear when the Cr concentration is increased to 18 at. %. On the other hand, the XRD Mn peak appears at a much higher dopant concentration of 30 at. % in the Mn-doped samples. These small XRD peaks represent clusters formed from a tiny percentage of dopant atoms below the detection limit of EXAFS. Formation of such clusters may indicate enhanced gathering of dopant atoms and therefore larger antiferromagnetic contribution to

the overall magnetization. The saturation magnetization for the Cr-doped samples started to decrease when the Cr concentration is increased to 18 at. % which is consistent with the XRD results. On the other hand, all the Mn samples studied in the present work have Mn concentration below 30 at. % so the effect of antiferromagnetic contribution is less conspicuous in the Mn-doped samples. Also, in contrast to the percolation of magnetic polarons model adopted for the Cr-doped samples,[8] the RKKY interaction is responsible for the ferromagnetism in the Mn-doped samples.[7] In the RKKY model, ferromagnetism largely depends on the carriers provided by the dopant atoms. Therefore, while increasing the number of antiferromagnetically coupled dopant atoms, the increase in Mn concentration may also give rise to an opposite magnetic effect, namely, enhancement of the carrier-mediated ferromagnetic interaction. In principle, the later can partially neutralize the relatively less conspicuous antiferromagnetic effect in the Mn-doped samples, leading to the observed level-off of magnetization decrease. Our present results have clearly excluded the possibility of dopant-dopant clusters and their direct exchange interaction as the major origin of above-250 K ferromagnetism in these amorphous Si magnetic semiconductor samples.

In conclusion, our experimental results have indicated successful incorporation of an unusually high concentration of Cr and Mn magnetic ions in hydrogenated amorphous Si thin films nearly free of Mn and Cr clusters and oxides. Antiferromagnetic coupling such as superexchange between magnetic ions can appear as their concentration increases to a certain level and therefore reduces the saturation magnetization. We propose that enhancement of carrier-mediated ferromagnetism in the Mn-doped samples may neutralize the effect of antiferromagnetic coupling, which is less conspicuous compared to that in the Cr-doped samples, and result in unchanged total magnetization. Our EXAFS results exclude the possibility of dominant formation of magnetic Cr and Mn clusters that can invalidate the proposed RKKY and magnetic polaron models, as well as potential technological applications, in the amorphous Si films.

*Author to whom correspondence should be addressed; soo@phys.nthu.edu.tw

[1] H. Munekata, H. Ohno, S. von Molnar, Armin Segmüller, L. L. Chang, and L. Esaki, Phys. Rev. Lett. **63**, 1849 (1989).

[2] H. Ohno, Science **291**, 840 (2001).

[3] Y. D. Park, A. T. Hanbicki, S. C. Erwin, C. S. Hellberg, J. M. Sullivan, J. E. Mattson, T. F. Ambrose, A. Wilson, G. Spanos, and B. T. Jonker, Science **295**, 651 (2002).

[4] J. Chen, K. L. Wang, and K. Galatsis, Appl. Phys. Lett. **90**, 012501 (2007).

[5] M. Bolduc, C. Awo-Affouda, A. Stollenwerk, M. B. Huang, F. G. Ramos, G. Agnello, and V. P. LaBella, Phys. Rev. B **71**, 033302 (2005).

[6] Li Zeng, A. Huegel, E. Helgren, F. Hellman, C. Piamonteze, and E. Arenholz, Appl. Phys. Lett. **92**, 142503 (2008).

[7] J.-H. Yao, H.-H. Lin, and T.-S. Chin, Appl. Phys. Lett. **92**, 242501 (2008).

[8] J.-H. Yao, S.-C. Li, M.-D. Lan, and T.-S. Chin, Appl. Phys. Lett. **94**, 072507 (2009).

[9] Y. L. Soo, S. C. Weng, W. H. Sun, S. L. Chang, W. C. Lee, Y. S.

Chang, J. Kwo, M. Hong, J. M. Ablett, C.-C. Kao, D. G. Liu, and J. F. Lee, Phys. Rev. B **76**, 132404 (2007).

[10] Y. L. Soo, S. W. Huang, Z. H. Ming, Y. H. Kao, H. Munekata, and L. L. Chang, Phys. Rev. B **53**, 4905 (1996).

[11] Y. L. Soo, G. Kioseoglou, S. Huang, S. Kim, Y. H. Kao, Y. Takatani, S. Haneda, and H. Munekata, Phys. Rev. B **63**, 195209 (2001).

[12] Y. L. Soo, Z. H. Ming, S. W. Huang, Y. H. Kao, R. N. Bhargava, and D. Gallagher, Phys. Rev. B **50**, 7602 (1994) and references cited therein.

[13] Y. L. Soo, G. Kioseoglou, S. Kim, S. Huang, Y. H. Kao, S. Kuwabara, S. Owa, T. Kondo, and H. Munekata, Appl. Phys. Lett. **79**, 3926 (2001).

[14] A. E. Kaloyeros, R. B. Rizk, and J. B. Woodhouse, Phys. Rev. B **38**, 13099 (1988).

[15] G. Dalba, P. Fornasini, R. Grisenti, F. Rocca, I. Chambouleyron, and C. F. O. Graeff, J. Phys.: Condens. Matter **9**, 5875 (1997).

[16] G. Ciatto, H. Renevier, M. G. Proietti, A. Polimeni, M. Capizzi, S. Mobilio, and F. Boscherini, Phys. Rev. B **72**, 085322 (2005).

[17] C. Bihler, G. Ciatto, H. Huebl, G. Martinez-Criado, P. J. Klar, K. Volz, W. Stolz, W. Schoch, W. Limmer, F. Filippone, A. Amore Bonapasta, and M. S. Brandt, Phys. Rev. B **78**, 235208 (2008).

[18] M. Newville, P. Līvins, Y. Yacoby, J. J. Rehr, and E. A. Stern, Phys. Rev. B **47**, 14126 (1993).

[19] J. J. Rehr, J. Mustre de Leon, S. I. Zabinsky, and R. C. Albers, J. Am. Chem. Soc. **113**, 5135 (1991).

[20] E. A. Stern, Phys. Rev. B **48**, 9825 (1993).

[21] P. Parikh, D. M. Bhardwaj, R. P. Gupta, N. L. Saini, S. Fernandes, R. K. Singhal, D. C. Jain, and K. B. Garg, Bull. Mater. Sci. **25**, 653 (2002).

[22] R. Gunnella, N. Pinto, L. Morresi, M. Abbas, and A. Di Cicco, J. Non-Cryst. Solids **354**, 4193 (2008).

[23] L. Zeng, E. Helgren, M. Rahimi, F. Hellman, R. Islam, B. J. Wilkens, R. J. Culbertson, and D. J. Smith, Phys. Rev. B **77**, 073306 (2008).

[24] G. S. Chang, E. Z. Kurmaev, D. W. Boukhvalov, L. D. Finkelstein, S. Colis, T. M. Pedersen, A. Moewes, and A. Dinia, Phys. Rev. B **75**, 195215 (2007).

[25] J. M. D. Coey, M. Venkatesan, and C. B. Fitzgerald, Nature Mater. **4**, 173 (2005).